Acta Mechanica Solida Sinica, Vol. 24, No. 4, August, 2011 ISSN 0894-9166
Published by AMSS Press, Wuhan, China

# NANOINDENTATION SIMULATION OF PE/POSS UNDER DIFFERENT SHAPES OF INDENTERS**

**Enlai Hu**[1] **Yi Sun**[1*] **Fanlin Zeng**[1] **Jianmin Qu**[2]

([1] *Department of Astronautic Science and Mechanics, Harbin Institute of Technology, Harbin* 150001*, China*)
([2] *Northwestern University, Department Civil & Environment Engineering, Evanston, IL* 60208 *USA*)

Received 19 February 2011; revision received 26 June 2011

**ABSTRACT** In this paper, the nanoindentation simulation on the two models of neat polyethylene (PE) and the polyethylene incorporated with 25wt% POSS (POSS-PE) is performed to reveal the reinforcing mechanism of the mechanical properties. The influence of the indenter shapes on nanoindentation is researched by using three different shapes of diamond indenters (cube-corner indenter, cylindrical indenter with spherical tip and cylindrical indenter with flat tip). The molecular mechanics method is adopted to eliminate the temperature effects. Under different indenters, the load-displacement responses, hardnesses (indentation hardness and Martens hardness) and Young's moduli of PE and POSS-PE are obtained. Compared with PE, all the mechanical properties are improved dramatically. Then, we analyze the source of loading drop phenomena and the enhancement mechanism of POSS. Furthermore, the result shows that the different shapes of indenters cause a large impact on indentation hardness, but a little impact on Martens hardness. And Young's modulus of the flat indenter is much larger than that of cube-corner indenter and spherical indenter.

**KEY WORDS** molecular simulation, nanoindentation, shape of indenter, hardness, Young's modulus

## I. INTRODUCTION

The organic-inorganic nano-hybrid materials are novel composite materials developed in recent years. With some particular modifiers, conventional organic materials can be modified to prepare new composite materials with special properties. Hybrid materials based on POSS are hot topics of research in the past few years[1–4]. They have wide potential applications in many engineering fields, such as automobile engineering, optical engineering and aeronautical engineering[5,6]. POSS is a class of multifunctional molecules (Fig.1). It is a cage of silicon and oxygen atoms having the formula $(RSiO_{3/2})_n$, where R is an inert organic group or active functional group. On the basis of different R groups, composite materials will generate corresponding characteristics. Among them, the mechanical properties, such as elastic modulus and hardness, are very important. Especially for thin membranes, hardness is almost an indispensable performance. In order to measure these properties of thin-film materials, the nanoindentation method is always performed[4,7–11]. For instance, Zeng[4] studied the hardness and size effect of polystyrene

* Corresponding author. E-mail: sunyi@hit.edu.cn

** Project supported by the National Natural Science Foundation of China (No. 10972066), the Doctoral Program Foundation of Institutions of Higher Education of China (No. 20070213054), the Natural Science Foundation of the Heilongjiang Province of China (A2007-10) and the Fundamental Research Funds for the Central Universities (No. HIT. NSRIF. 2010070).

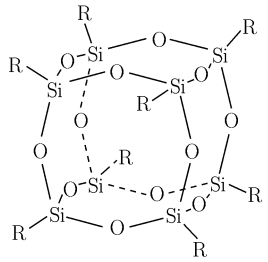

Fig. 1. Illustration the typical POSS monomer structure.

incorporated with POSS under a square indenter by using molecular simulations. Jeng[8] simulated the nanoindentation process of Cu thin-film covered by polymers, with a triangular pyramid indenter. Wahab[9] and Lee[11] researched thin polymers films by nanoindentation tests. However, for these tests, the deformation details on the atomic scale could not be observed, and the hardness under little indenter depth is difficult to explore. In addition, little attention is focused on the atomic deformation mechanism of polymers since different indenters may lead to different results in nanoindentation. Hence in this paper, three indenters are adopted to conduct the nanoindentation simulations of PE and POSS-PE. We first analyze the enhancement mechanism of POSS, and then compare the influence of the sharps of indenters on hardness and Young's modulus.

## II. MODELS AND SIMULATION DETAILS

Strain loading is adopted in the nanoindentation. As shown in Fig.2, the whole model contains two parts. The top part A is the cube-corner indenter. Part B is the sample to test, and the bottom of B named C is fixed. The same strain is loaded on the indenter step by step. The models of neat PE, POSS-PE and diamond indenter are built. The PE model includes 32 molecular chains. Each chain contains 498 $CH_2$ groups and 2 $CH_3$ groups. The total atom number of the model is 48064. The density is 0.904 g/cm$^3$ and the initial sizes are $a = 69.5410$ Å, $b = 72.2955$ Å, $c = 84.5242$ Å; $\alpha = 86.5212$, $\beta = 88.8148$, $\gamma = 103.920$. The POSS-PE model contains 32 molecular chains (Fig.3). Each chain is built with 3 POSS monomers and straight-chain PE. The total atom number is 56896. The density is 0.97 g/cm$^3$ and the initial sizes are $a = 85.9529$ Å, $b = 71.6145$ Å, $c = 91.2180$ Å; $\alpha = 99.5949$, $\beta = 84.9095$, $\gamma = 72.7355$. In this paper, three kinds of typical diamond indenters are adopted, such as, cube-corner indenter, cylindrical indenter with spherical tip and cylindrical indenter with flat tip. The cube-corner indenter consists of 3469 atoms. The sphere indenter contains 3889 atoms and the diameter is 30 Å. The flat indenter includes 4439 atoms and the diameter is also 30 Å. The nanoindentation models as shown in Figs.4(a) and 4(b), are made up of the three indenters, the PE model and the POSS-PE model, respectively.

In the simulations, the COMPASS[12] force field is employed to describe the interactions between atoms. First, the optimal structures of the models are obtained by using the conjugate gradient method. The atoms of the indenter and the bottom of the sample are then fixed. After that, the indenter is started to impress under strain loading step by step. And the equilibrium states are obtained through enough relaxation at each step. Gradually load up to a certain degree, and then unload step by step. Thus, the

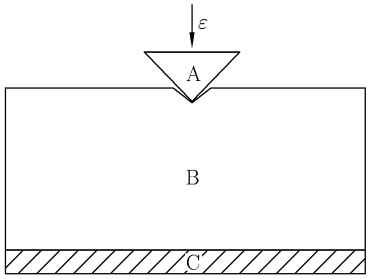


Fig. 2. The indentation model.

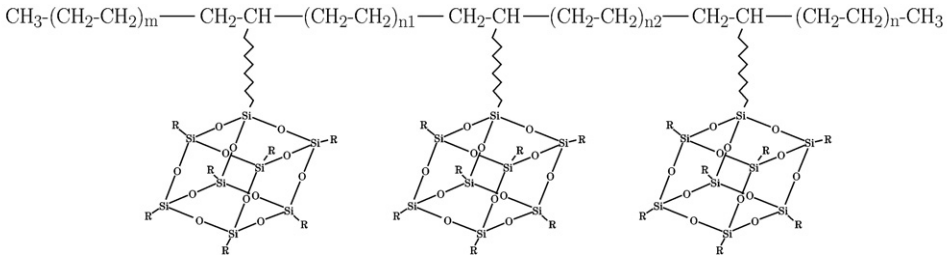

Fig. 3. The POSS-PE molecular chain.

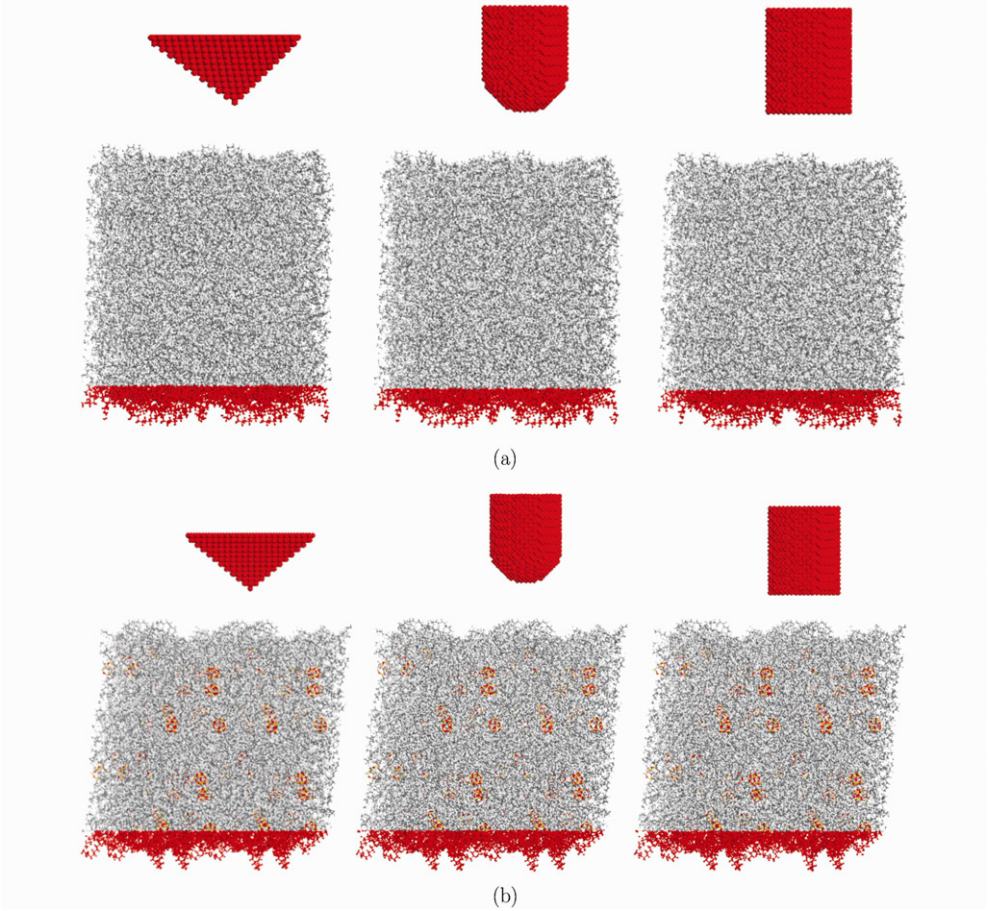

Fig. 4. (a) The initial indentation models of PE (from left to right, the indenter tips were cube-corner, sphere, flat); (b) The initial indentation models of POSS-PE (from left to right, the indenter tips were cube-corner, sphere, flat).

atomic motion trajectories of the models under loading and unloading processes are received. Note in the loading versus displacement curve, the displacement is the movement distance of the indenter, and the force is the total interaction force between indenter and sample. In all the simulations, the indenter is ideal, i.e., its shape and size remains fixed. For the models, the displacement of indenter per step is 0.25 Å, and the total displacement is about 20 Å.

## III. RESULTS AND DISCUSSIONS

### 3.1. Load-displacement Response

From the simulations of the nanoindentation, the deformation processes of the two models are visible. With the aids of the indent loading and its displacement, the loading-depth curves of PE and POSS-PE under three different indenters are depicted in Figs.5(a) and 5(b), respectively. And the curves of

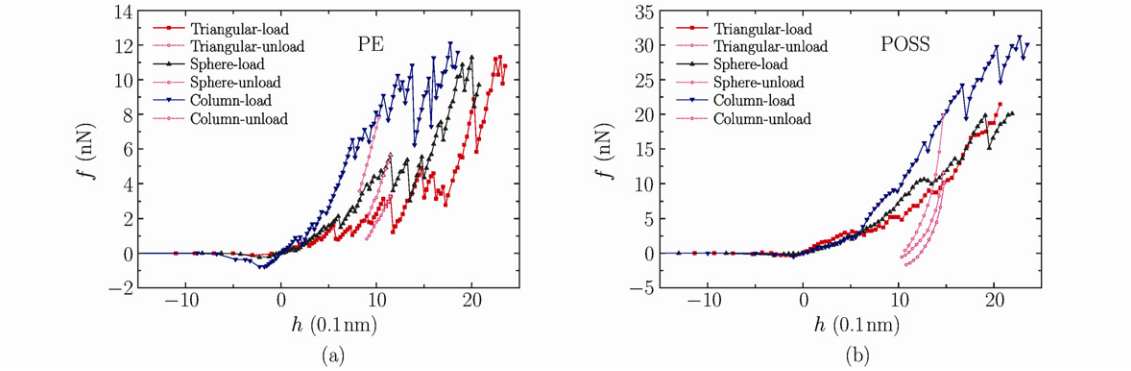


Fig. 5. (a) The load-depth curves of PE; (b) The load-depth curves of POSS-PE.

the three indenters are in agreement with the data of different indenters in Ref.[13]. Figure 5 shows the forces of the POSS-PE model are much larger than that of PE, which represents the deformation resistibility of POSS-PE is stronger than that of PE. In other words, the resistance of PE is enhanced by incorporating POSS. In addition, several loading drop phenomena (or strain bursts) are observed clearly from the three loading curves in Fig.5(a). This is consistent with Refs.[14,15]. For metal crystal, it is believed that the main source of loading drop is collective nucleation or dislocation avalanches[14]. Similarly, note that the slipping near the indenter tip maybe is the most important factor in load drop phenomena for polymers. For the sake of simplicity, the slipping of two paralleled molecular chains of PE is investigated. As the parallel relationship of the two chains, the slipping force and distance is obtained directly. And then the slipping work $W_s$ is calculated. Moreover, the external work $W_e$ and the increment of potential energy $\Delta U$ must follow the law of conservation of energy, i.e.,

$$W_e + W_s = \Delta U + U_c \tag{1}$$

Where, $U_c$ is the error caused by the simulation and calculation process. The calculation result shows that all the values of $U_c/\Delta U$ seem negligible (less than 2.8%). Consequently, Eq.(1) could be rewritten as follows:

$$W_s = \Delta U - W_e \tag{2}$$

As shown in Eq.(2), owing to the external work $W_e$ being a positive value, the source of the drop of potential energy ($\Delta U < 0$) is that slipping consumes relatively more energy. Namely, slipping leads to loading drop. Moreover, Eq.(2) shows that the slipping energy could be obtained via nanoindentation simulation. The slipping energy of PE at each step is calculated by Eq.(2) and shown in Fig.6. Each loading drop is corresponding to a certain protrudent slipping energy, i.e., the slipping occurs while the load drops. Therefore, the loading drop phenomena are mainly caused by the slipping between molecular chains.

However, the loading drop reduces obviously in Fig.5(b), compared with Fig.5(a). This should be due to the less slipping in the POSS-PE model, which means the slipping between molecular chains of

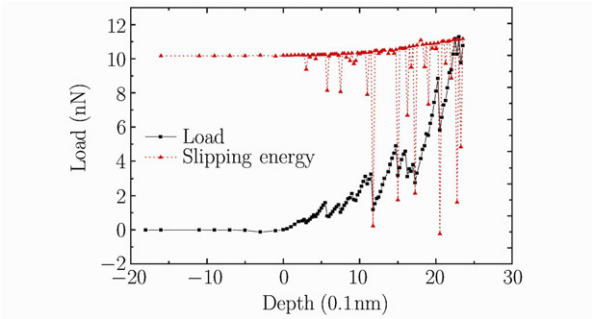


Fig. 6. Slipping-load relation of PE in nanoindentation.

PE is suppressed by POSS. The critical reason is that the POSS monomer itself posses a cage structure (Fig.1), which provides high stability and large volume. Thereby, it is difficult to deform, move and rotate for the POSS monomer. In this case, the local area of POSS is restricted by constraints. Thus, the slipping between PE molecular chains is suppressed by POSS.

### 3.2. Hardness and Young's Modulus

Figure 5 shows that the contact force of the indenter is nearly zero when the indenter is far from the substrate. And the force changes from attraction to repulsion as the distance shortens. In the process, there is a critical value (when the force equals to zero), which is defined as the initial zero position. Then, the contact depth is confirmed. Since the shape of the indenter is fixed, the contact area and the projected area could be calculated approximately through the contact depth. And the contact loading equals the resultant force of the indenter due to Newton's third law. In general, two kinds of hardness are defined on the basis of the two areas (contact area $A_c$ and projected area $A_p$). One is the indentation hardness[9, 16, 17] given by

$$H = \frac{P}{A_p} \tag{3}$$

and the other is Martens hardness[18] given by

$$H = \frac{P}{A_c} \tag{4}$$

According to Eq.(3), the indentation hardness of PE and POSS-PE under different indenters are described in Fig.7. It's clearly observed that only the hardness of the cube-corner indenter decreases and converges with the increasing depth; while the hardness of the spherical indenter and the flat indenter shows a rising trend, and the values of them are obviously larger than that of the cube-corner indenter in the later period. This is consistent with the data reported in Ref.[19]. The reason is that the projected area of the flat indenter is a constant, and that of the sphere indenter tends to a constant. Their indentation hardness keeps rising with the increasing load. One possible reason to cause this phenomenon is the large friction between the indenter and the substrate.

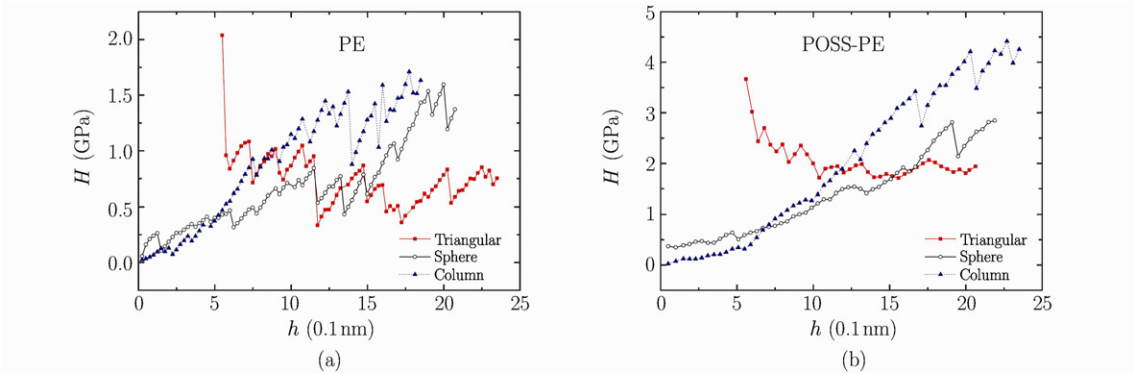


Fig. 7. (a) The indentation hardness of PE; (b) The indentation hardness of POSS-PE.

Martens hardness of PE and POSS-PE under different indenters are calculated by Eq.(4) and shown in Fig.8. Unlike the indentation hardness, Martens hardness under the three different indenters converges to the same value. Actually, the three indenter tips all act on the same area of the same model. Thus, it is reasonable that the three curves tend to the same value. And the hardness of PE is in accord with Ref.[20]. In other words, Martens hardness eliminates the influence of the shape of indenters. The result indicates Martens hardness is much more befitting for PE and POSS-PE in this paper. In addition, it's inferred that Martens hardness also is more suited to the nanoindentation with large friction between the indenter and the substrate. Furthermore, both the indentation hardness and Martens hardness of POSS-PE displayed in Figs.7 and 8 are much larger than those of PE for each indenter. Therefore, incorporated with POSS, the mechanical properties of PE are greatly improved.

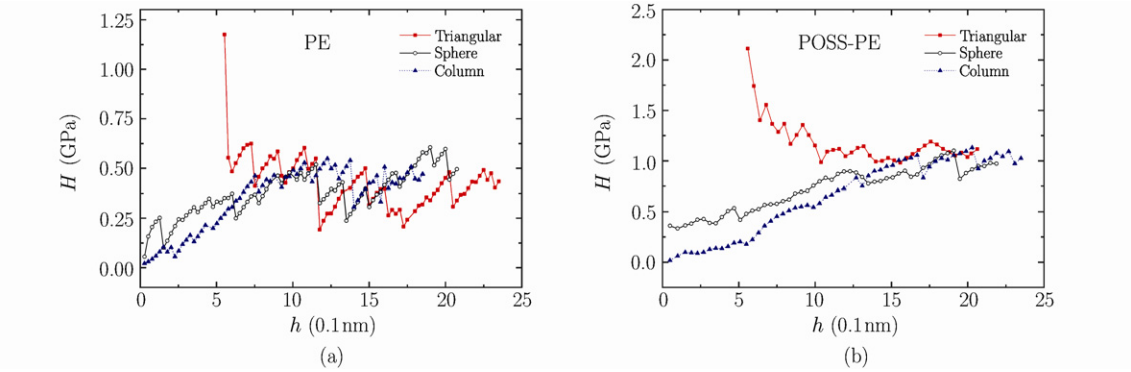


Fig. 8. (a) Martens hardness of PE; (b) Martens hardness of POSS-PE.

Through fitting the curves of Fig.8, Martens hardness of PE and POSS-PE under different indenters are listed in Table 1. Based on Oliver and Pharr[16] method, their Young's moduli are obtained from the unloading curves of Fig.5.

$$E_r = \frac{\sqrt{\pi}}{2\beta}\frac{S}{\sqrt{A}} \tag{5}$$

where, $\beta$ is the dimensional parameter related to the shape of the indenter ($\beta = 1.05$ for cube-corner indenter, $\beta = 1$ for spherical indenter and flat indenter[17], $A$ is the projected area, and $S$ is the unloading stiffness given by

$$S = \left(\frac{\mathrm{d}P}{\mathrm{d}h}\right)_{h=h_{\max}} = Bm(h_{\max} - h_f)^{m-1} \tag{6}$$

where, $h_{\max}$ is the maximum depth, $h_f$ is the final depth after the indenter is fully unloaded. $B$ and $m$ are power law fitting constants. From Eq.(7), $B$ and $m$ could be obtained by fitting the data of the upper portion of the unloading curve during the initial stage of unloading.

$$P = B(h - h_f)^m \tag{7}$$

Table 1. **Martens hardness and Young's modulus of PE and POSS-PE**

| Model | Martens hardness (GPa) | | | Young's modulus (GPa) | | |
|---|---|---|---|---|---|---|
| | Cube-corner | Sphere | Flat | Cube-corner | Sphere | Flat |
| PE | $0.42 \pm 0.05$ | $0.44 \pm 0.09$ | $0.45 \pm 0.05$ | 5.40 | 5.68 | 8.05 |
| POSS-PE | $1.08 \pm 0.06$ | $0.98 \pm 0.08$ | $1.02 \pm 0.07$ | 24.12 | 21.76 | 33.20 |

As shown in Table 1, the values of Young's moduli of PE are consistent with Ref.[21]. Clearly, for each indenter, Martens hardness and Young's modulus of POSS-PE are much larger than those of PE. And the enhancement effect is similar to that of POSS on polypropylene in Ref.[22]. The result indicates that the mechanical properties of PE improve obviously by POSS. In addition, for the cube-corner indenter and spherical indenter, the values of Young's moduli have little difference. However, the value of Young's modulus for the flat indenter is much larger. The main reason of the large difference in Young's modulus includes 2 factors. One is that there is high stress concentration at the edge of the bottom of the flat indenter, and it changes obviously during the unloading process. But the stress concentrations are not significant for the other two indenters. Another is that the size of the indenter is too small due to the limitation of the capabilities of computers. So it is difficult to eliminate the stress concentration. Thus, the unloading curves are influenced obviously by the stress concentration. In other words, Young's modulus obtained from the unloading curves contains the impact of stress concentration at the edge of the indenters.

## IV. CONCLUSIONS

In this paper, we adopt molecular mechanics method to simulate the nanoindentation behaviors of two models of PE and POSS-PE. Three different shapes of diamond indenters (cube-corner indenter, cylindrical indenter with spherical tip and cylindrical indenter with flat tip) are employed. The load-displacement responses, hardness (indentation hardness and Martens hardness) and Young's modulus of PE and POSS-PE are obtained. Comparing the load of PE model with that of POSS-PE under the same depths, the result shows that the mechanical properties of PE increase dramatically by POSS. Then, the enhancement mechanism of POSS is analyzed. Because the POSS itself has a three-dimensional structure of space with a big volume, besides the structure is steady and hard to deform. The deformation and slipping of molecular chains near POSS monomer are suppressed, which leads to the enhancement by POSS. In addition, loading drop phenomena of load-displacement curves are analyzed. The major cause is the slipping of molecular chains around the indenter tip. From the curves of the indentation hardness and Martens hardness, it is found that the different shapes of indenters cause a large impact on indentation hardness, but a little impact on Martens hardness. This implies that Martens hardness applies to the nanoindentation with large friction between the indenter and the substrate. Moreover, Young's moduli of different indenters indicate that Young's modulus of the flat indenter is much larger than that of the cube-corner indenter and spherical indenter, due to the impact of stress concentration at the edge of indenters.

## References


[1] Peng,Y. and Mccabe,C., Molecular simulation and theoretical modeling of polyhedraloligomeric silsesquioxanes. *Molecular Physics*, 2007, 105: 261-272.

[2] Tsuchida,A. and Bolln,C. et al., Ethene and propene copolymers containing silsesquioxane side groups. *Macromolecules*, 1997, 30: 2818-2824.

[3] Li,G.Z. and Wang,L.C. et al., Polyhedral oligomeric silsesquioxane (POSS) polymers and copolymers: A review. *Journal of Inorganic and Organometallic Polymers*, 2001, 11: 123-154.

[4] Zeng,F.L., Sun,Y., Zhou,Y. and Li,J., Molecular mechanics simulation on the nanoindentation on POSS nanocomposite. *Proceedings of SPIE*, 2007, 6423: 642322.

[5] Dodiuk,H. and Kenig,S. et al., Nanotailoring of epoxy adhesives by polyhedral-oligomeric-sil-sesquioxanes (POSS). *International Journal of Adhesion & Adhesives*, 2005, 25: 211-218.

[6] Pielichowski,K. and Njuguna,J., Polyhedral oligomeric silsesquioxane (POSS) containing nanohybrid polymers. *Advances in Polymer Science*, 2006, 201: 225-296.

[7] Zeng,F.L., Sun,Y., Zhou,Y. and Li,Q.K., A molecular dynamics simulation study to investigate the elastic properties of PVDF and POSS nanocomposites. *Modelling and Simulation in Materials Science and Engineering*, 2011, 19: 025005.

[8] Jeng,Y.R., Tsai,P.C. and Liu,Y.H., Adsorbed multilayer effects on the mechanical properties in nanometer indentation depth. *Materials Research Bulletin*, 2009, 44: 1995-1999.

[9] Wahab,M.A., Mya,K.Y. and He,C.B., Synthesis, morphology, and properties of hydroxyl terminated-POSS/polyimide low-k nanocomposite films. *Journal of Polymer Science: Part A: Polymer Chemistry*, 2008, 46: 5887-5896.

[10] Zeng,F.L. and Sun,Y., Quasicontinuum simulation of nanoindentation of nickel film. *Acta Mechanica Solida Sinica*, 2006, 19(4): 283-288.

[11] Lee,H.J., Hur,S. and Han,S.W. et al., The mechanical properties of thin polymer film for nanoimprinting lithography by nanoindentation. *Nanotechnology*, 2003, 2: 546-549.

[12] Sun,H., COMPASS: An ab initio force-field optimized for condensed-phase applications-overview with details on alkane and benzene compound. *Journal of Physical Chemistry B*, 1998, 102: 7338-7364.

[13] Lu,Y.C. and Shinozaki,D.M., Characterization and modeling of large displacement micro-/nano-indentation of polymeric solids. *Journal of Engineering Materials and Technology-Transactions of the Asme*, 2008, 130(4): 041001.1-041001.7.

[14] Csikor,F.F., Motz,C. and Weygand,D. et al., Dislocation avalanches, strain bursts, and the problem of plastic forming at the micrometer scale. *Science*, 2007, 312(5848): 251-254.

[15] Feng,G. and Ngan,A.H.W., Creep and strain burst in indium and aluminium during nanoindentation. *Scripta Materialia*, 2001, 45: 971-976.

[16] Oliver,W.C. and Pharr,G.M., An improved technique for determining hardness and elastic-modulus using load and displacement sensing indentation experiments. *Journal of Materials Research*, 1992, 7(6): 1564-1583.

[17] Oliver,W.C. and Pharr,G.M., Measurement of hardness and elastic modulus by instrumented indentation: Advances in understanding and refinements to methodology. *Journal of Materials Research*, 2004, 19(1): 3-20.

[18] Shahdad,S.A. and McCabe,J.F. et al., Hardness measured with traditional Vickers and Martens hardness methods. *Dental Materials*, 2007, 23: 1079-1085.

[19] Xue,Z., Huang,Y., Hwang,K.C. and Li,M., The influence of indenter tip radius on the micro-indentation hardness. *Journal of Engineering Materials and Technology*, 2002, 124(3): 371-379.

[20] Yashiro,K., Furuta,A. and Tomita,Y., Nanoindentation on crystal/amorphous polyethylene: Molecular dynamics study. *Computational Materials Science*, 2006, 38(1): 136-143.

[21] Bischel,M.S. and Vanlandingham,M.R. et al., On the use of nanoscale indentation with the AFM in the identification of phases in blends of linear low density polyethylene and high density polyethylene. *Journal of Materials Science*, 2000, 35(1): 221-228.

[22] Misra,R., Fu,B.X. and Morgan,S.E., Surface energetics, dispersion, and nanotribomechanical behavior of POSS/PP hybrid nanocomposites. *Journal of Polymer Science Part B: Polymer Physics*, 2007, 45(17): 2441-2455.